Stochastically gated diffusion model of selective nuclear transport

Paul C. Bressloff

Phys. Rev. E **101**, 042404 — Published 13 April 2020

DOI: 10.1103/PhysRevE.101.042404

"Stochastically-gated" diffusion model of selective nuclear transport

Paul C. Bressloff
Department of Mathematics, University of Utah 155 South 1400 East, Salt Lake City, UT 84112

Nuclear pore complexes (NPCs) allow the selective exchange of molecules between the cytoplasm and cell nucleus. Although small molecules can diffuse freely through an NPC, the transport of proteins and nucleotides requires association with transport factors (kaps). The latter transiently bind to disordered flexible polymers within the NPC, known collectively as phenylalanine-glycine-nucleoporins (FG-Nups). It is has recently been shown that transient binding combined with diffusion in the bound state is a sufficient mechanism for selective transport. However, selectivity is significantly reduced if the mobility of the bound state is too slow. In this paper we formulate the binding-diffusion mechanism of selective transport in terms of a "stochastically-gated" diffusion process in which each bound particle undergoes confined diffusion within a subdomain of the NPC. This allows us to make explicit the fact that the diffusion of a particle when bound to a polymer tether is spatially confined rather than simply reduced. We calculate the selectivity of the NPC, and explore its dependence on the size of the confinement domains. We then use probabilistic methods to determine the splitting probability and mean first passage time (MFPT) for an individual particle to pass through the pore. Our analysis establishes that spatial confinement can significantly reduce selectivity in a binding-diffusion model, suggesting that other biophysical mechanisms such as interchain transfer are required.

I. INTRODUCTION

The nucleus of eukaryotes is surrounded by a protective nuclear envelope within which are embedded nuclear pore complexes (NPCs). The NPCs are the sole mediators of exchange between the nucleus and cytoplasm. In general small molecules of diameter ~ 5 nm can diffuse through the NPCs unhindered, whereas larger molecules up to around 40 nm in diameter are excluded unless they are bound to a family of soluble protein receptors known as karyopherins (kaps), see the reviews [1–4]. Within the cytoplasm kap receptors bind cargo to be imported via a nuclear localization signal (NLS) that results in the formation of a kap-cargo complex. This complex can then pass through an NPC to enter the nucleus, where a small enzyme RanGTP binds to the kap, causing a conformational change that releases the cargo. The sequence of events underlying the import of cargo is shown in Fig. 1(a). In the case of cargo export from the nucleus, kaps bind to cargo with a nuclear export signal (NES) in the presence of RanGTP, and the resulting complex passes through the NPC. Once in the cytoplasm, RanGTP is hydrolyzed by the cytoplasmic factor RanGAP1 to form RanGDP, resulting in the release of the cargo. The export process is illustrated in Fig. 1(b). Finally, RanGDP is recycled to the nucleus by another molecule NFT2 and is reloaded with GTP to begin another import/export cycle. The conversion to RanGTP is mediated by a chromatin-associated guanine exchange factor RanGEF. This cycle allows a single NPC to support a very high rate of transport on the order of 1000 translocations/sec and a typical transit time of $\sim$ 10 ms [5]. Since the transportation cycle is directional and accumulates cargo against a concentration gradient, an energy source combined with a directional cue is required. Both of these are provided by the hydrolysis of RanGTP and the maintenance of a concentration gradient of RanGTP across the NPC. The RanGTP gradient is continuously regenerated by GTP hydrolysis in the cytoplasm, translocation of RanGTD into the nucleus by NFT2, and replacement of GDP by GTP in the nucleus. It is important to note that the energy generated from RanGTP hydrolysis is ultimately used to create a concentration gradient of RanGTP between the nucleus and cytoplasm, so that the actual translocation across the NPC occurs purely via diffusion.

Although the above basic picture is now reasonably well accepted, the detailed mechanism underlying facilitated diffusion of kap-cargo complexes within the NPC is still not understood. The NPC is composed of about 30 distinct proteins known collectively as nucleoporins (Nups). It has emerged in recent years that individual Nups are directly related to a number of human diseases including influenza and cancers such as leukemia [6], as well as playing an important role in viral infections by providing docking sites for viral capsids [7]. Associated with many of the Nups are natively unfolded phenylalanine-glycine (FG) repeats, known collectively as FG-Nups [8, 9]. The FG-Nups set up a barrier to diffusion for large molecules so that the key ingredient in facilitated diffusion through the NPC is the interaction between kap receptors with the FG-Nups. In essence, the major difference between most theoretical models of NPC transport concerns the built in assumptions regarding the properties and spatial arrangements of FG-Nups within the NPC, and the nature of interactions with kaps during translocation through the NPC [4, 10]. One important feature that emerges from the various theoretical studies is that kap complexes should also be mobile in the bound state.

Two complementary approaches to modeling the interior of an NPC are based on polymer brushes and polymer gels, respectively. The former treats the FG-Nups as flexible polymer tethers to which kaps can temporarily

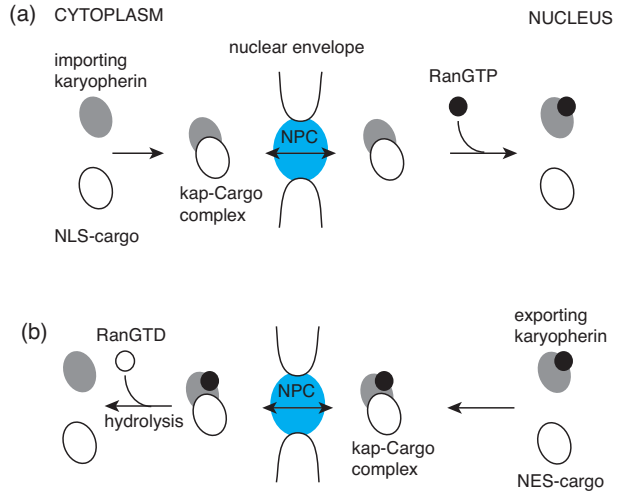

FIG. 1. Schematic illustration of the (a) import and (b) export process underlying the karyopherin-mediated transportation of cargo between the nucleus and cytoplasm via a nuclear pore complex (NPC). See text for details.

bind and undergo confined diffusion in the bound state [11–13]. The mechanical properties of the tethers contribute to the effective diffusivity of the complexes in the bound state. It is also possible that complexes undergo interchain transfers without unbinding (sliding) [8]. The other type of model treats the NPC as a weakly reversible gel [5, 14–16]. A gel is a jelly-like material that is mostly liquid by weight, yet behaves like a solid due to a 3D cross-linked polymer network within the liquid. (A gel is said to be reversible if the crosslinking is reversible.) Particles smaller than the mesh size of the network can diffuse freely through the NPC, whereas non-selective macromolecules larger than the mesh size cannot. On the other hand, kap-cargo complexes can 'dissolve' in the gel due to the presence of hydrophobic domains on the surface of the kap receptors, and then diffuse through the pore by breaking the weak bonds of the reversible gel [5, 14, 17]. Alternatively, one can treat the gel as a continuum of binding sites for kap complexes, with the gel properties determining the effective diffusivity in the bound state [18].

A number of recent modeling studies have included more details concerning the binding interactions between kap complexes and FG-Nupss [11–13, 18]. Consider, in particular, the binding-diffusion model of Maguire *et al.* [13]. This is a minimal one-dimensional (1D) model of selective transport in which kap-cargo complexes (particles) randomly switch between a freely-diffusing state and a more slowly diffusing state in which the particle is bound to an FG-Nup tether. The FG-Nups are assumed to be uniformly distributed along the pore at some fixed concentration. Combining numerical simulations with analytical results in the low binding limit, the authors show how transient tethered diffusion can lead to significant selectivity.

In this paper, we show how the binding-diffusion mechanism can be mapped on to a model of stochastically gated diffusion, analogous to the case of an array of cells coupled by stochastically-gated gap junctions [19, 20], and use this to calculate the selectivity of a nuclear pore. The basic assumption of the model is that the FG-Nups are distributed in clusters in such a way that they define confinement domains. This then allows us to make explicit the fact that the diffusion of a particle when bound to a tether is spatially confined rather than simply reduced (at least in the absence of sliding). The structure of the paper is as follows. In section II we introduce the model and show how it relates to the model of Ref. [13]. We also highlight the analogy with stochastically gated diffusion through gap junctions. In section III we explicitly calculate the selectivity of the model pore, and explore its parameter dependence. We also compare our results with those of Ref. [13]. Finally, in section IV we use probabilistic methods previously developed in Refs. [20] to determine the mean first passage time (MFPT) for an individual particle to pass through the pore.

II. BINDING-DIFFUSION MODEL

Consider diffusing particles (kap-complexes) moving through a 1D pore of length $L_{\rm tot} = ML$, which is partitioned into M domains of size L, see Fig. 2(a). Let $x \in [(j-1)L, jL]$, $j = 1, \ldots, M$, denote the spatial coordinates of the j-th domain. Suppose that a cluster of FG-Nups is tethered at the center $x = (j-1/2)L$ of each domain $j = 1, \ldots, M$. The FG-Nups are flexible polymers that act as transient, partially mobile traps for the diffusing particles. This has two consequences. First, a particle can potentially bind to an FG-Nup anywhere in a given domain. For simplicity, we take the binding rate to be independent of the current location of the head of an FG-Nup, which is reasonable if the effective reaction radius is sufficiently large. Thus one can treat the binding sites within a domain as spatially uniform. Second, in the bound state the complex continues to diffuse within the domain, but cannot escape it. That is, each cluster defines a confinement domain of size L. As an additional simplification, we do not include any potential energy contributions to the stochastic motion of the bound complex, other than it is confined to the given domain.

Denote the state of a freely diffusing particle by $n = 0$ and the state of a bound particle by $n = 1$. Let $U(x,t)$ and $V(x,t)$ be the concentration of particles in the states $n = 0$ and $n = 1$, respectively. Let $N_{\rm tot}$ denote the uniform concentration of FG-Nup binding sites. The corresponding two-state reaction-diffusion equations are

$$\frac{\partial U}{\partial t} = D_0 \frac{\partial^2 U}{\partial x^2} - (N_{\rm tot} - V) k_{\rm on} U + k_{\rm off} V \quad (2.1a)$$

$$\frac{\partial V}{\partial t} = D_1 \frac{\partial^2 V}{\partial x^2} + (N_{\rm tot} - V) k_{\rm on} U - k_{\rm off} V, \quad (2.1b)$$

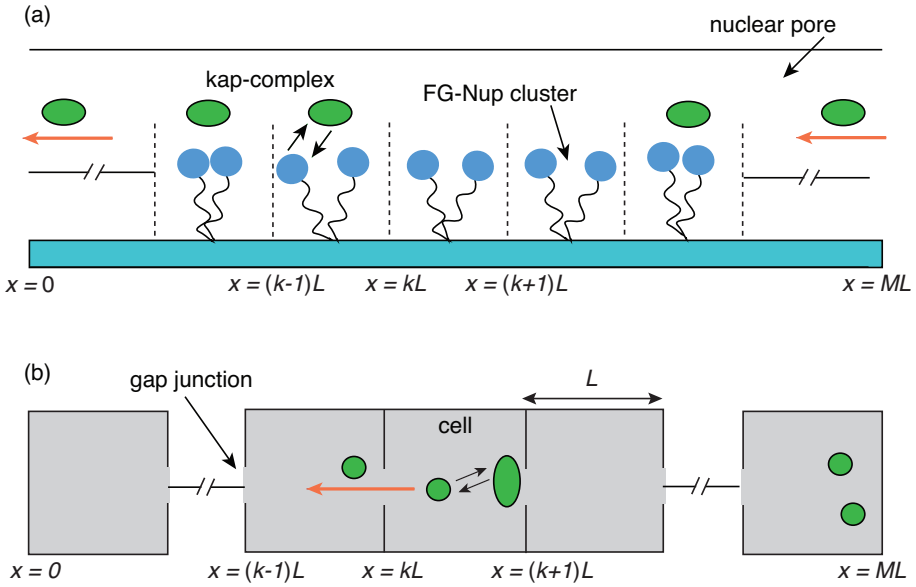

FIG. 2. Examples of stochastically-gated diffusion. (a) Binding-diffusion model of selective transport in a nuclear pore. Each particle (kap-complex) switches between a freely diffusing state ($n = 0$) and a bound state ($n = 1$) in which it is tethered to an FG-Nup cluster. The latter state has a smaller diffusivity ($D_1 < D_0$) and is confined to a domain of size L. (b) 1D array of cells of size L coupled by gap junctions. Diffusing particles randomly switch between two different conformational states labeled $n = 0, 1$ and can only pass through a gap junction when in the state $n = 0$.

where $N_{\rm tot} - V$ is the concentration of unbound FG-Nup binding sites, $k_{\rm on}$ and $k_{\rm off}$ are the binding and unbinding rates, and D_n is the diffusivity of a particle in state n, with $D_0 \geq D_1$. We will assume that a bound particle cannot escape the NPC, whereas an unbound particle is free to enter or leave the NPC. Moreover, the external concentration of freely diffusing particles on either side of the NPC is fixed. Hence, the external boundary conditions are given by

$$U(0,t) = 0, \quad \partial_x V(0,t) = 0,$$
$$U(L_{\rm tot},t) = \eta, \quad \partial_x V(L_{\rm tot},t) = 0. \tag{2.2}$$

As they stand, Eqs. (2.1) and (2.2) are identical in form to those considered in Ref. [13]. The one major difference in our model is that bound particles are confined to a domain of size L associated with a given cluster of FG-Nups. This means that we also have to impose interior boundary conditions. These take the form

$$[U(x)]_{x=L_j^-}^{x=L_j^+} = 0, \quad [\partial_x U(x)]_{x=L_j^-}^{x=L_j^+} = 0 \tag{2.3a}$$
$$\partial_x V(L_j^-) = 0 = \partial_x V(L_j^+). \tag{2.3b}$$

Eqs. (2.3a) ensure continuity of the concentration and flux across the point $x = L_j = jL$ when the particle is freely-diffusing, whereas the reflecting boundary conditions (2.3b) implement the constraint that a bound particle attached to a tethered FG-Nup cannot switch to a neighboring domain. (This condition could be weakened by incorporating sliding.)

For analytical tractability, we will focus on the weak binding regime for which $N_{\rm tot} - V \approx N_{\rm tot}$ and the effective binding rate is the constant $N_{\rm tot}k_{\rm on}$. The model defined by Eqs. (2.1), (2.2) and (2.3) is then formally similar to a model of a 1D array of cells coupled by gap junctions [19, 20], see Fig. 2(b). Suppose that diffusing particles within the cytoplasm of a cell randomly switch between two conformational states, $n = 0, 1$, and can only pass through a gap junction to an adjoining cell if it is in the state $n = 0$. Thus each cell acts as a confinement domain when a particle is in the state $n = 1$. The selective transport model can be mapped on to the gap junction model by reinterpreting U (V) as the concentration of diffusing molecules in conformational state $n = 0$ ($n = 1$), and replacing $k_{\rm on}$ and $k_{\rm off}$ by the rates of switching between the two states. One major difference between the two models is the length-scale, with $L_{\rm tot} \sim 100$ nm for a nuclear pore and $L \sim 1 - 100\mu m$ for a cell. A second difference is that the diffusivity in the two conformational states is approximately the same for gap-junction transport [21].

In this paper we will assume parameter values similar to those considered in Ref. [13]. In particular, we will take $D_0 = 0.12\mu{\rm m}^2/{\rm s}$, $D_1/D_0 \sim 0.05 - 1$, $k_{\rm on} = 10^3\mu M^{-1}\ {\rm s}^{-1}$, $K \equiv k_{\rm off}/k_{\rm on} \sim 10^{-2} - 10^3\mu{\rm M}^{-1}$, $N_T = 4.7{\times}10^3\mu$M , and $L_{\rm tot} = 0.1\mu$m. Note that binding is ultrafast [22].

III. CALCULATION OF SELECTIVITY

We are interested in calculating the steady-state flux at the end $x = 0$ and comparing it to pure diffusion in

order to determine the selectivity of the nuclear pore. (This is analogous to calculating the effective permeability in an array of cells coupled by stochastically-gated gap junctions [19, 20].) Following Ref. [13], we perform the change of variables $\widehat{V} = V - N_{\rm tot}K_AU$, with $K_A = K^{-1} = k_{\rm on}/k_{\rm off}$ the binding equilibrium constant. The steady-state version of Eqs. (2.1) can then be rewritten as

$$0 = D_0\frac{d^2U}{dx^2} + k_{\rm off}\widehat{V}, \tag{3.1a}$$

$$0 = D_1\frac{d^2\widehat{V}}{dx^2} - k_{\rm off}\widehat{V} + N_{\rm tot}K_AD_1\frac{d^2U}{dx^2}. \tag{3.1b}$$

Substituting for $k_{\rm off}\widehat{V}$ in equation (3.1b) using equation (3.1a) leads to the fourth-order equation

$$\frac{d^4U}{dx^4} = \lambda^2\frac{d^2U}{dx^2}, \quad \lambda^2 = \frac{k_{\rm off}D_0 + N_{\rm tot}k_{\rm on}D_1}{D_0D_1}. \tag{3.2}$$

The general solution in the j-th domain is thus of the form (U_j, V_j), $j = 1, \ldots, M$, with

$$U_j(x) = a_j + b_j[x - x_{j-1}] + c_j{\rm e}^{\lambda[x-x_{j-1}]} + d_j{\rm e}^{-\lambda[x-x_{j-1}]} \tag{3.3}$$

and

$$V_j(x) = N_{\rm tot}K_AU_j(x) - \frac{D_0}{k_{\rm off}}\frac{d^2U_j}{dx^2}, \quad x \in (x_{j-1}, x_j), \tag{3.4}$$

with the coefficients a_j, b_j, c_j, d_j determined by the boundary conditions at the endpoints $x_{j-1} = (j-1)L$ and $x_j = jL$. The latter can be rewritten as

$$U_j(x_j) = U_{j+1}(x_j), \quad U_j'(x_j) = U_j'(x_j) \tag{3.5a}$$

$$V_j'(x_{j-1}) = 0 = V_j'(x_j). \tag{3.5b}$$

Imposing the continuity conditions (3.5a) yields

$$a_j + b_jL + c_j{\rm e}^{\lambda L} + d_j{\rm e}^{-\lambda L} = a_{j+1} + c_{j+1} + d_{j+1}, \tag{3.6a}$$

$$b_j + \lambda c_j{\rm e}^{\lambda L} - \lambda d_j{\rm e}^{-\lambda L} = b_{j+1} + \lambda c_{j+1} - \lambda d_{j+1}. \tag{3.6b}$$

Similarly, the no-flux conditions (3.5b) give

$$N_{\rm tot}K_A(b_j + \lambda(c_j - d_j)) - \frac{D_0\lambda^3}{k_{\rm off}}(c_j - d_j) = 0, \tag{3.6c}$$

$$N_{\rm tot}K_A\left(b_j + \lambda\left(c_j{\rm e}^{\lambda L} - d_j{\rm e}^{-\lambda L}\right)\right) - \frac{D_0\lambda^3}{k_{\rm off}}\left(c_j{\rm e}^{\lambda L} - d_j{\rm e}^{-\lambda L}\right) = 0 \tag{3.6d}$$

Combining Eqs. (3.6c,d) shows that

$$\lambda(c_j - d_j) = \lambda\left(c_j{\rm e}^{\lambda L} - d_j{\rm e}^{-\lambda L}\right) = \Gamma_0 b_j, \tag{3.7}$$

and $d_j = -{\rm e}^{\lambda L}c_j$, with

$$\Gamma_0 = \left[\frac{D_0\lambda^2}{k_{\rm off}N_{\rm tot}K_A} - 1\right]^{-1} = \frac{N_{\rm tot}k_{\rm on}D_1}{k_{\rm off}D_0} \tag{3.8}$$

for all $j = 1, \ldots, M$, It then follows from Eq. (3.6b) that $b_j = B$ and, hence,

$$c_j = \frac{\Gamma_0}{\lambda({\rm e}^{\lambda L}+1)}B, \quad d_j = -\frac{\Gamma_0}{\lambda(1+e^{-\lambda L})}B \tag{3.9}$$

for all $j = 1, \ldots, M$. Finally, substituting for b_j, c_j and d_j in Eq. (3.6a), we have the iterative equation

$$a_{j+1} = a_j + \left(L + \frac{2\Gamma_0\left[{\rm e}^{\lambda L} - 1\right]}{\lambda({\rm e}^{\lambda L}+1)}\right)B \equiv a_j + \mathcal{R}B,$$

that is,

$$a_{j+1} = a_1 + j\mathcal{R}B, \quad 1 \le j < M - 1. \tag{3.10}$$

There remain two unknowns, namely a_1 and B. These are determined by the exterior boundary conditions (2.2) for U:

$$U_1(0) = 0, \quad U_M(ML) = \eta.$$

The latter yield the pair of equations

$$a_1 + \frac{\Gamma_0(1 - {\rm e}^{\lambda L})}{\lambda(1+{\rm e}^{\lambda L})}B = 0$$

$$a_1 + (M-1)\mathcal{R}B + BL + \frac{\Gamma_0\left[{\rm e}^{\lambda L} - 1\right]}{\lambda({\rm e}^{\lambda L}+1)}B = \eta,$$

which can be rearranged to give

$$a_1 = \frac{\Gamma_0}{\lambda}\tanh(\lambda L/2)B, \tag{3.11}$$

with

$$B = \frac{\eta}{M}\left(L + \frac{2\Gamma_0}{\lambda}\tanh(\lambda L/2)\right)^{-1}. \tag{3.12}$$

Finally, the flux out of the end $x = 0$ is

$$J = D_0\frac{\partial U}{\partial x}\bigg|_{x=0} = U_1'(0) = D_0(1+\Gamma_0)B. \tag{3.13}$$

Substituting for B and setting $L = L_{\rm tot}/M$, the flux can be written as

$$J = \frac{\eta D_0}{M}(1+\Gamma_0)\left(\frac{L_{\rm tot}}{M} + \frac{2\Gamma_0}{\lambda}\tanh(\lambda L_{\rm tot}/2M)\right)^{-1}, \tag{3.14}$$

with Γ_0 given by Eq. (3.8). In order to determine the selectivity of the pore, we need to compare J with the flux J_0 of freely diffusing particles,

$$J_0 = \frac{\eta D_0}{L_{\rm tot}}. \tag{3.15}$$

The selectivity is then defined according to $S = J/J_0$, which is independent of η (in the low binding limit). Note that in the limit $k_{\rm on} \to 0$, we have $\Gamma_0 \to 0$ and $S \to 1$.

We would like to compare the selectivity of our model with that of Ref. [13], which corresponds to the case $M = 1$. (After some algebra, it can be shown that if $M = 1$, then Eq. (3.14) reduces to the expression for the flux obtained in Ref. [13].) For concreteness, we will assume that all parameters are fixed at their base values (as specified at the end of section II), except for $K = k_{\rm off}/k_{\rm on}$, $\Delta = D_1/D_0$ and M. We also set $S = S(K, \Delta, M)$. One way to characterize the difference between the two models is as follows. We take $\Delta \approx 1$ and impose a hard limit on the confinement region of a bound particle so that $M > 1$. On the other hand, Maguire *et al.* [13] take $M = 1$ and incorporate a soft version of confinement by modeling each bound molecule as a Brownian particle diffusing in a harmonic potential well; this then implies that $\Delta < 1$ ($D_1 < D_0$). More specifically, the position $X(t)$ of a bound particle relative to the center of the well evolves according to the Langevin equation

$$dX = -\frac{kX(t)}{\gamma} + \sqrt{2D_0}dW(t), \tag{3.16}$$

where $W(t)$ is a Wiener process, and γ is a friction coefficient with $D_0\gamma = k_BT$. The spring constant k is estimated by treating the polymer as a worm-like chain [23], that is, $k = 3k_BT/2\ell_pL_c$, where ℓ_p is the persistence length of the polymer and L_c is its contour length. Solving the corresponding Fokker-Planck equation for $X(0) = 0$ yields the mean-square displacement (MSD) [13]

$$\langle X^2(t)\rangle = \frac{1 - {\rm e}^{-2kD_At/k_BT}}{k/k_BT}.$$

However, one also has to take into account the fact that the probability density of being bound for a time t is

$$\rho(t) = \tau^{-1}{\rm e}^{-t/\tau}, \quad \tau = \frac{1}{k_{\rm off}},$$

so that the effective MSD is

$$\overline{\langle X^2\rangle} = \int_0^\infty \rho(t')\langle X^2(t')\rangle dt' = \frac{2D_0L_c\ell_p}{L_c\ell_pk_{\rm off} + 3D_0}. \tag{3.17}$$

after using the explicit formula for the spring constant k. The diffusivity D_1 is then estimated by treating the confined diffusion over the mean bound time τ as Fickian, that is [13],

$$D_1 = \frac{\overline{\langle X^2\rangle}}{2\tau} = \frac{D_0}{1 + 3D_0/D_p}, \tag{3.18}$$

where $D_p = L_c\ell_pk_{\rm off}$ quantifies how the physical properties of the polymer determine the diffusivity in the bound state. In particular, mobility in the bound state increases with increasing chain length L_c or persistence length ℓ_p, and decreases with increasing binding lifetime $k_{\rm off}^{-1}$. For large D_p it can be seen that D_1 approaches the free diffusivity D_0, whereas $D_1 \ll D_0$ when D_p is small.

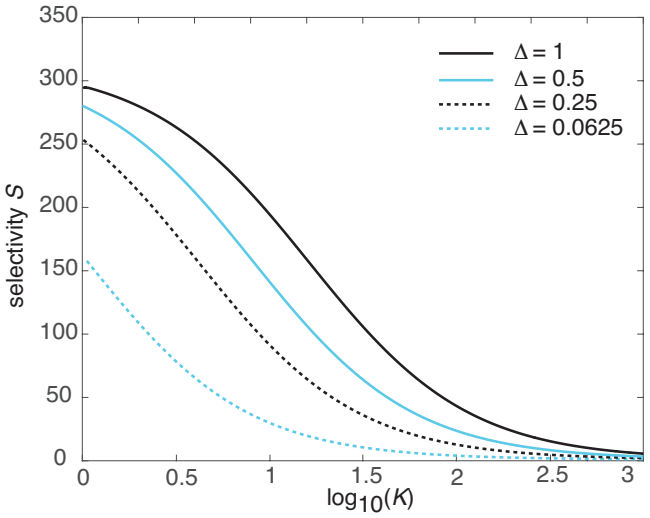

FIG. 3. Plot of selectivity $S = S(K, \Delta, 1)$ as a function of the dissociation constant $K = k_{\rm off}/k_{\rm on}$ for various values of $\Delta = D_1/D_0$. Other parameters specified at the end of section II.

One central result of Ref. [13] is that for fixed K the selectivity is a maximum when $D_0 = D_1$. However, if the soft confinement by FG-Nup tethers is taken into account, then $D_1 < D_0$ and selectivity is reduced. This suggests that taking $D_1 = D_0$, say, and increasing M should also reduce selectivity, and this is precisely what we find. In Fig. 3 we plot the selectivity $S(K, \Delta, 1)$ as a function of K for various values of Δ, $0 < \Delta \leq 1$. This recovers the results of Ref. [13] in the low binding regime. Similarly, in Fig. 4 we plot $S(K, 1, M)$ as a function of K for various values of M, $M \geq 1$. Compar-

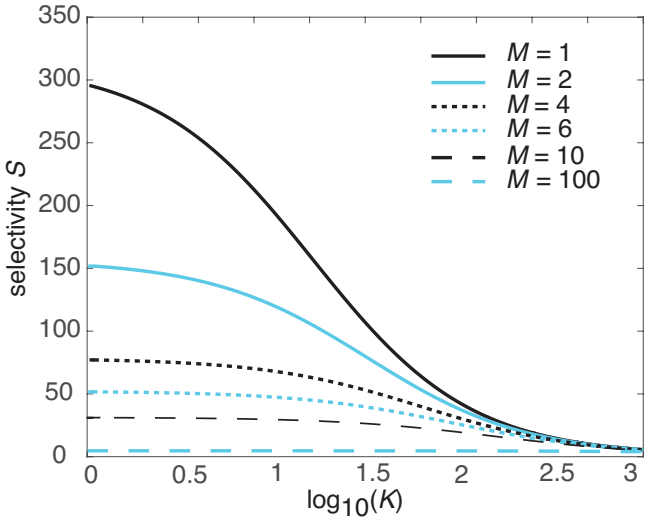

FIG. 4. Plot of selectivity $S = S(K, 1, M)$ as a function of the dissociation constant $K = k_{\rm off}/k_{\rm on}$ for various values of $M = L_{\rm tot}/L$. Other parameters specified at the end of section II.

ison of the two figures shows that hard confinement has a much stronger effect then soft confinement in terms of reducing selectivity. Note that this argument holds even though we have restricted our analysis to the low binding regime by taking $K \geq 1$ in Figs. 3 and 4. If nonlinearities associated with the saturation of binding sites were included, then the system of equations would have to be solved numerically. As shown in Ref. [13] for $M = 1$ and $D_1 \approx D_0$, the selectivity curves are unimodal, with a peak around $K = 1$ and $S \to 0$ as $K \to 0$. The latter limit is a consequence of the fact that when $K \to 0$, particles cannot unbind from FG-Nups, which thus act as permanent traps. Hence particles cannot exit the NPS and the selectivity vanishes. This argument also holds for $M > 1$. Moreover, it is clear from Fig. 4 that the selectivity curves for $M > 1$ have reached a maximum at $K = 1$, and will thus decrease to zero in the domain $K < 1$. In other words, restricting our analysis to the low binding regime is sufficient to identify the maximum possible selectivity of the diffusion-binding model with hard confinement.

The assumption of low binding also arises in other models of the NPC. For example, consider the entropic (virtual) gating model [2, 24], which takes into account the fact that macromolecules diffusing in a confined geometry (such as a nuclear pore) experiences an entropic barrier due to excluded volume effects. Within the NPC this would be enhanced by the densely packed FG-Nups. One way to counteract the effects of the entropic barrier is for the kaps to have an affinity for and bind to the FG-repeat regions, thus lowering the effective free energy of the cargo-complex within the NPC. The degree of affinity has to be sufficiently high to overcome the entropic barrier but not too high otherwise the complex can be trapped within the NPC and the rate of translocation would be too small. One possible solution, is to have a large number of low–affinity binding sites within the nuclear pore. Mathematically speaking, this can be modeled in terms of diffusion through an effective energy landscape, which approximates the effects of multiple binding sites when the binding/unbinding rates are relatively fast compared to the diffusion rate [24].

IV. FIRST PASSAGE TIME FOR A SINGLE PARTICLE

So far we have considered the diffusion of many particles through the nuclear pore. Here we follow a complementary single-particle perspective, and use probabilistic arguments previously developed for gap junctions [20] in order to investigate the splitting probability and MFPT for a particle to exit a pore. We assume that the particle exits the pore at $x = 0$ or $x = L$ only when $n(t) = 0$, otherwise it is reflected. We also set $D_1 = D_0$ and focus on the effect of varying M.

A. Splitting probabilities

Let $X(t) \in [0, L_{\rm tot}]$ denote the position of the particle at time t and define the stopping time

$$T = \inf\big\{t \geq 0 : \{X(t) \in \{0, L_{\rm tot}\}\} \cap \{n(t) = 0\}\big\}. \tag{4.1}$$

This is the FPT for the particle to reach either external boundary and is in the freely diffusing state $n(t) = 0$, so that it is absorbed by the boundary (exits the pore). For $n \in \{0, 1\}$, introduce the splitting probability that the particle is absorbed at the left-hand boundary $x = 0$ given that $X(0) = x$ and $n(0) = n$:

$$\pi_n(x) = \mathbb{P}(X(T) = 0 \,|\, \{X(0) = x\} \cap \{n(0) = n\}). \tag{4.2}$$

From the backward two-state diffusion equation, one finds that π_n satisfies [20]

$$0 = D_0 \frac{d^2\pi_0}{dx^2} - N_{\rm tot} k_{\rm on} \pi_0 + N_{\rm tot} k_{\rm on} \pi_1 \tag{4.3a}$$

$$0 = D_0 \frac{d^2\pi_1}{dx^2} + k_{\rm off} \pi_0 - k_{\rm off} \pi_1, \tag{4.3b}$$

with exterior boundary conditions

$$\pi_0(0) = 1, \quad \pi_0(L_{\rm tot}) = 0, \quad \pi_1'(0) = 0, \quad \pi_1'(L_{\rm tot}) = 0,$$

and interior boundary conditions

$$\pi_0(L_j^-) = \pi_0(L_j^+),\ \pi_0'(L_j^-) = \pi_0'(L_j^+),$$
$$\pi_1'(L_j^-) = \pi_1'(L_j^+) = 0.$$

Recall that $L_j = jL = jL_{\rm tot}/M$. Suppose that $\mathbb{P}[n(0) = n] = \rho_n$ and set $p_n(x) := \rho_n \pi_n(x)$ with

$$p_n(x) = \mathbb{P}(\{X(T) = 0\} \cap \{n(0) = n\} \,|\, X(0) = x),$$

and

$$\rho_0 = \frac{k_{\rm off}}{k_{\rm off} + N_{\rm tot} k_{\rm on}}, \quad \rho_1 = 1 - \rho_0.$$

That is, ρ_0 is the stationary probability that the particle is in the freely diffusing state. The p_n satisfy

$$0 = D_0 \frac{d^2 p_0}{dx^2} - N_{\rm tot} k_{\rm on} p_0 + k_{\rm off} p_1 \tag{4.4a}$$

$$0 = D_0 \frac{d^2 p_1}{dx^2} + N_{\rm tot} k_{\rm on} p_0 - k_{\rm off} p_1, \tag{4.4b}$$

with modified exterior boundary conditions

$$p_0(0) = \rho_0, \quad p_0(L_{\rm tot}) = 0, \quad p_1'(0) = 0, \quad p_1'(L_{\rm tot}) = 0,$$

and the same interior boundary conditions as π_n.

From the definition of p_n, we have

$$p(x) := p_0(x) + p_1(x) = \mathbb{P}(X(T) = 0 \,|\, X(0) = x).$$

By the strong Markov property [25], if $0 \le j \le M-1$ and $x \in (L_j, L_{j+1})$, then

$$p(x) = \frac{1}{\rho_0}\Big(q(s)p_0(L_j) + (1-q(s))p_0(L_{j+1})\Big), \quad (4.5)$$

where $s = x - L_j$, $q(s)$ is the splitting probability that the particle first exits (L_j, L_{j+1}) at the left-hand boundary,

$$q(s) = \mathbb{P}(X(\tau_k) = L_j \,|\, X(0) = s), \quad (4.6)$$

and τ_k is the stopping time for the particle to first exit the interval (L_j, L_{j+1}):

$$\tau_j = \inf\big\{t \ge 0 : \{X(t) \notin (L_j, L_{j+1})\} \cap \{n(t) = 0\}\big\}. \quad (4.7)$$

Eq. (4.5) can be understood as follows. The splitting probability $p(x)$ with $x \in (L_j, L_{j+1})$ can be decomposed into the sum of (i) the probability $q(s)$ that the particle first escapes the interval at L_j times the probability $\pi_0(L_j)$ that it is subsequently absorbed at $x = 0$ starting from $x = L_j$ in the unbound state, and (ii) the probability $1 - q(s)$ that the particle first escapes the interval at L_{j+1} times the probability $\pi_0(L_{j+1})$ that it is subsequently absorbed at $x = 0$ starting from $x = L_j$ in the unbound state.

The calculation of $q(s)$ is equivalent to obtaining the splitting probability of a particle in $[0, L]$ escaping at the end $x = 0$ first. One finds that

$$q(x) = \frac{\rho_0\xi(L-x) + e^{\xi L}(\rho_0([L-x]\xi - 1) + 1) + \rho_0 - 1}{\rho_0(L\xi + 2) + e^{\xi L}(\rho_0(L\xi - 2) + 2) - 2}, \quad (4.8)$$

where

$$\xi = \sqrt{\frac{N_{\rm tot}k_{\rm on} + k_{\rm off}}{D_0}}.$$

Note from Eq. (3.2) that $\lambda = \xi$ when $D_1 = D_0$. In the case of ultrafast binding, which occurs within the NPC, we have $\xi L \gg 1$ so that

$$q(x) \approx \frac{\rho_0(\xi[L-x] - 1) + 1}{\rho_0(L\xi - 2) + 2}.$$

Since $p_0(0) = \rho_0$, $p_0(L_{\rm tot}) = 0$, it follows that $p(x)$ is determined by the remaining $M-1$ constants $p_0(L_1), \ldots, p_0(L_{M-1})$. As the domains are evenly spaced, we find that each of these constants is the average of its neighbors [20]

$$p_0(L_j) = \frac{1}{2}\big(p_0(L_{j-1}) + p_0(L_{j+1})\big), \quad (4.9)$$

for $j = 1, \ldots, M-1$. Rearranging (4.9), we see that the constants satisfy a discretized Laplace's equation

$$p_0(L_{j-1}) - 2p_0(L_j) + p_0(L_{j+1}) = 0, \quad (4.10)$$

for $j = 1, \ldots, M-1$, with boundary conditions $p_0(0) = \rho_1$, $p_0(L_{\rm tot}) = 0$. Solving this system and applying (4.5) yields $p(x)$.

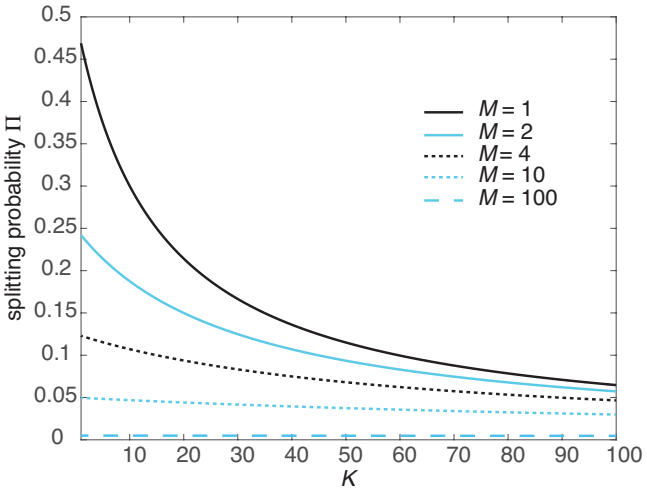

FIG. 5. Plot of splitting probability as a function of the dissociation constant $K = k_{\rm off}/k_{\rm on}$ for various values of M and $D_1 = D_0$. Other parameters as in Fig. 4.

Analogous to the analysis of selectivity in section III, consider the splitting probability $\Pi = p(L_{\rm tot})$ for reaching the end $x = 0$ having started at $x = L_{\rm tot}$. From Eq. (4.5) we see that

$$\Pi = \frac{q(L_{\rm tot}/M)}{\rho_0}p_0(L_{M-1}), \quad (4.11)$$

where $L_{M-1} = L_{\rm tot}[1 - M^{-1}]$. Iterating Eq. (4.10), we find that

$$p_0(L_{M-1}) = \frac{\rho_0}{M}.$$

That is, starting from $j = M-1$ and using $\rho(L_M) = 0$, we have

$$p(L_{M-2}) - 2p_0(L_{M-1}) = 0,$$
$$p(L_{M-3}) - 2p(L_{M-2}) + p(L_{M-1}) = 0,$$

from which we deduce $p(L_{M-2}) = 2p(L_{M-1})$ and $p(L_{M-3}) = 3p(L_{M-1})$. Iterating this procedure and using $p(L_0) = \rho_0$ yields the result. In conclusion

$$\Pi = \frac{q(L_{\rm tot}/M)}{M}. \quad (4.12)$$

In Fig. 5 we plot the splitting probability as a function of the dissociation constant for various M. Consistent with the analysis of selectivity in section III, reducing the size of the confinement domain (increasing M) reduces the probability that the particle reaches the end $x = 0$.

B. Mean first passage times

In order to investigate how confinement affects the time to exit a pore, we will calculate the expected absorption time (MFPT) of the particle to exit either of

the ends $X = 0, L_{\rm tot}$ starting at the center of the pore. Defining the stopping time

$$T_n(x) = \inf\big\{t \geq 0 : \{X(t) \in \{0, L_{\rm tot}\}\} \cap \{n(t) = 0\} \,|\, \{X(0) = x\} \cap \{n(0) = n\}\big\}, \tag{4.13}$$

the corresponding MFPT is

$$\omega_n(x) = \mathbb{E}[T_n(x)]. \tag{4.14}$$

The analysis of $\omega_n(x)$ proceeds along similar lines to the splitting probability. First, one can show that w_n satisfies the ODEs [20]

$$-\rho_0 = D\frac{d^2 w_0}{dx^2} - N_{\rm tot} k_{\rm on} w_0 + k_{\rm off} w_1 \tag{4.15a}$$

$$-\rho_1 = D\frac{d^2 w_1}{dx^2} + N_{\rm tot} k_{\rm on} w_0 - k_{\rm off} w_1, \tag{4.15b}$$

with exterior boundary conditions

$$w_0(0) = 0 \quad w_0(L_{\rm tot}) = 0, \quad w_1'(0) = 0 \quad w_1'(L_{\rm tot}) = 0,$$

and the same interior boundary conditions as π_n.

Let $w(x) = w_0(x) + w_1(x)$. By the strong Markov property [25], if $0 \leq j \leq M-1$ and $x \in (L_j, L_{j+1})$, then

$$w(x) = v(s) + \frac{1}{\rho_0}\Big(q(s) w_0(L_j) + (1 - q(s)) w_0(L_{j+1})\Big), \tag{4.16}$$

where $s = x - L_j$, $v(x)$ is the mean exit time to escape the interval (L_j, L_{j+1}) starting at s, and the splitting probability $q(s)$ is given in (4.8). We can calculate $v(x)$ by considering the MFPT for a particle to escape from either end in the interval $[0, L]$:

$$v(x) = \frac{1}{2}\Big(x(L-x) + \frac{L\rho_1 \coth\left(\frac{L\xi}{2}\right)}{\rho_0 \xi}\Big). \tag{4.17}$$

Since $w_0(0) = w_0(L_{\rm tot}) = 0$, it remains to determine the $M-1$ constants $w_0(L_1), \ldots, w_0(L_{M-1})$. For evenly spaced domains, we find that [20]

$$w_0(L_j) = V + \frac{1}{2}\big(w_0(L_{j-1}) + w_0(L_{j+1})\big) \tag{4.18}$$

for $j = 1, \ldots, M-1$, where V is the MFPT to escape from an interval of length $2L$ starting at the center of the domain and $n(0) = 0$:

$$V = \frac{L\left(L\rho_0\xi + 2\rho_1 \tanh\left(\frac{L\xi}{2}\right)\right)}{2\xi}. \tag{4.19}$$

Rearranging (4.18), we notice that these constants satisfy a discretized Poisson equation

$$w_0(L_{j-1}) - 2w_0(L_j) + w_0(L_{j+1}) = -2V \tag{4.20}$$

for $j = 1, \ldots, M-1$, and $w_0(0) = w_0(L_{\rm tot}) = 0$ can be interpreted as boundary conditions.

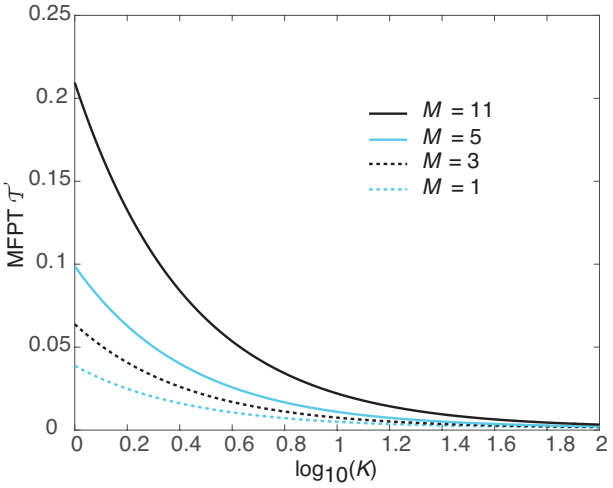

FIG. 6. Plot of MFPT $\mathcal{T}$ as a function of the dissociation constant $K = k_{\rm off}/k_{\rm on}$ for various values of M and $D_1 = D_0$. Other parameters are as in Fig. 4.

Set $\mathcal{T} = w(L_{\rm tot}/2)$ and take M to be odd so that the point $L_{\rm tot}$ lies at the center of the interval $[L_{[M-1]/2}, L_{[M+1]/2}]$. Equation (4.16) implies that

$$\mathcal{T} = v(L/2) + \frac{1}{\rho_0} q(L/2) w_0(L_{[M-1]/2}) + \frac{1}{\rho_0}(1 - q(L/2)) w_0(L_{[M+1]/2}). \tag{4.21}$$

Iterating Eq. (4.20) and using the boundary condition $\omega_0(L_{\rm tot}) = 0$ establishes that

$$\omega_0(L_{M-r}) = r\omega_0(L_{M-1}) - r(r-1)V, \quad 1 < r < M.$$

Setting $r = M$ and using $\omega_0(0) = 0$, gives

$$\omega_0(L_{M-1}) = (M-1)V,$$

and hence

$$\omega_0(L_{M-r}) = r(M-r)V, \quad 1 < r \leq M. \tag{4.22}$$

Substituting into Eq. (4.21), we have

$$\mathcal{T} = v(L_{\rm tot}/2M) + \frac{V}{4\rho_0}(M^2 - 1) \quad M \geq 1. \tag{4.23}$$

In Fig. 6 we plot the MFPT $\mathcal{T}$ as a function of the dissociation constant for various values of M. It can be seen that in the absence of confinement ($M = 1, D_0 = D_1$) the MFPT is a decreasing function of K and is of the order of msec over the whole range of K. (This is consistent with time-scales observed experimentally [22].) However, for fixed K, the MFPT is an increasing function of M so that fast transport requires K to be large. Comparison of Fig. 6 with Figs. 4 and 5 also shows another important feature of binding-diffusion models, namely that increasing the dissociation constant reduces the MFPT but at the cost of reducing selectivity. This makes sense, since more time is spent in the unbound state.

V. DISCUSSION

In this paper we formulated the binding-diffusion mechanism of selective nuclear transport in terms of a stochastically-gated diffusion process, in which each bound particle undergoes confined diffusion within a subdomain of the NPC. We showed analytically that hard confinement can significantly reduce selectivity and increase the time to pass through a nuclear pore. This suggests that the minimal binding-diffusion model needs to be supplemented by additional biophysical mechanisms in order to counter the effects of confinement.

One possible candidate is a so-called sliding mechanism, whereby additional mobility in the bound state arises from multivalent interactions, which allow transfer of particles between polymer chains while remaining bound [8, 26]. For example, a particle may bind simultaneously to more than one FG-Nup, and move hand-over-hand while remaining bound. Thus particles slide between nearby FG-Nup sites rather than fully unbinding and rebinding. The effects of interchain transfer has been investigated numerically using the binding-diffusion model with soft confinement [13]. In particular, diffusion in a harmonic potential is supplemented by hopping between neighboring FG-Nup sites, and numerical simulations are used to estimate the MSD and thus the effective bound diffusivity D_1. As expected, the inclusion of interchain transfer increases D_1 and thus enhances selectivity. In future work we will explore how to incorporate biophysical mechanisms such as interchain transfer into the stochastically-gated diffusion model. Another extension would be to take into account the elastic properties of the tether; this could either reduce the bound diffusivity D_1 along the lines of [13], but could also facilitate transport as suggested by Fogelson and Keener [12].

One remaining issue is how one could determine whether hard confinement ($D_1 \approx D_0$ and $M > 1$) or soft confinement ($D_1 < D_0$ and $M = 1$) is a more realistic description of FG-Nup/kap interactions (in the absence of sliding). There are a number of qualitative differences between the two cases, as highlighted in Figs. 3 and 4. First, decreasing D_1 displaces the selectivity peak to smaller values of the dissociation constant $K = k_{\rm off}/k_{\rm on}$, whereas the selectivity curves flatten out around $K = 1$ for all M. Second, the reduction of D_1 in the soft-confinement model depends on the unbinding rate $k_{\rm off}$, as illustrated by Eq. (3.18). That is, the particle only experiences the harmonic potential when it is bound to an FG-Nup. On the other hand, the size of a confinement domain is determined by the effective length and distribution of FG-Nups, but is independent of $k_{\rm off}$. One experimental test would be to image the precise motion of individual particles within the NPC using single particle tracking, say, and seeing whether the motion of bound particles is better described by confined diffusion or by normal diffusion with a reduced diffusion coefficient. One way to distinguish between the two cases would be to plot the mean-squared displacement as a function of time. However, such measurements could be confounded by particles switching between bound and unbound states, and by the sliding of bound particles to neighboring FG-Nups. Another issue concerns the distribution of FG-Nups within the NPC. One of the simplifications of the hard confinement model is to partition the NPC into a set of equal-size confinement domains, based on the assumption that FG-Nups are themselves regularly spaced (possibly in clusters). Having a random distribution of FG-Nups could be one way to "soften" the confinement. Irrespective of which precise version of diffusion-binding is more realistic, it is clear that switching between bound and unbound diffusing states provides a simple mechanism for enhancing selectivity of the NPC, provided that the binding affinity is not too small nor too large.

ACKNOWLEDGEMENTS

PCB was supported by the National Science Foundation (DMS-1613048 and IOS-1755431).

[1] I. G. Macara. Transport into and out of the nucleus. Microbiol. Mol. Biol. Rev. **65** 570-594 (2001).
[2] M. P. Rout, J. D. Aitchison, M. O. Magnasco, and T. B. Chait. Virtual gating and nuclear transport: The hole picture. Trends Cell Biol **13** 622-628 (2003).
[3] E. J. Tran and S. R. Wente. Dynamic nuclear pore complexes: Life on the edge. Cell **125** 1041-1053 (2006).
[4] T. Jovanovic-Talisman and A. Zilman. Protein transport by the nuclear pore complex: simple biophysics of a complex biomachine. Biophys. J. **113** 6-14 (2017).
[5] K. Ribbeck and D. Gorlich. Kinetic analysis of translocation through nuclear pore complexes. EMBO J **21** 2664-2671 (2001).
[6] J. M. Cronshaw and M. J. Matunis. The nuclear pore complex: disease associations and functional correlations. Trends Endocrinol. Metab. **15** 34-39 (2004).
[7] G. R. Whittaker, M. Kann and A. Helenius. Viral entry into the nucleus. Annu. Rev. Cell Dev. Biol. **16** 627-651 (2000).
[8] B. Raveh, J. M. Karp and D. Cowburn. Slide-and-exchange mechanism for rapid and selective transport through the nuclear pore complex. Proc. Natl. Acad. Sci. USA. **113** E2489-E2497 (2016).
[9] H. B. Schmidt and D. Gorlich. Transport selectivity of nuclear pores, phase separation, and membraneless organelles. Trends Biochem. Sci. **41** 46-61 (2016).
[10] A. Becskei and I. W. Mattaj. Quantitative models of nuclear transport. Curr. Opin. Cell Biol. **17** 27-34 (2005).
[11] B. Fogelson and J. P. Keener. Enhanced nucleocytoplasmic transport due to competition for elastic binding sites.

Biophys. J. **115** 108-116 (2018).

[12] B. Fogelson and J. P. Keener. Transport facilitated by rapid binding to elastic tethers. SIAM J. Appl. Math. **79** 1405-1422 (2019).

[13] L. Maguire, M. Stefferson, M. D. Betterton and L. E. Hough. Design principles of selective transport through biopolymer barriers. Phys. Rev. E **100** 042414 (2019).

[14] K. Ribbeck and D. Gorlich. The permeability barrier of nuclear pore complexes appears to operate via hydrophobic exclusion. EMBO J **21** 2664-2671 (2002).

[15] T. Bickel and R. Bruinsma. The nuclear pore complex mystery and anomalous diffusion in reversible gels. Biophys J. **83** 3079–3987 (2002).

[16] T. Kustanovich and Y. Rabin. Metastable network model of protein transport through nuclear pores. Biophys J. **86** 2008-2016 (2004).

[17] C. P. Goodrich, M. P. Brenner, and K. Ribbeck. Enhanced diffusion by binding to the crosslinks of a polymer gel. Nat. Comm. **9** 4348 (2018).

[18] Y. J. Yang, D. J. Mai, T. J. Dursch and B. D. Olsen. Nucleopore-inspired polymer hydrogels for selective biomolecular transport. Biomacromolecules **19** 3905-3916 (2018).

[19] P. C. Bressloff. Diffusion in cells with stochastically-gated gap junctions. SIAM J. Appl. Math. **76** 1658-1682 (2016).

[20] P. C. Bressloff, and S. D. Lawley. Diffusion on a tree with stochastically-gated nodes. J. Phys. A **49** 245601 (2016).

[21] An alternative version of the gap junction model is to treat each gap junction as a stochastic gate that randomly switches between an open and closed state; a particle can only pass through the gap junction when it is open. This is a much more complicated problem because all of the particles are diffusing in the same randomly switching environment, which introduces higher-order statistical correlations. Moreover, if the gates switch independently then the environment exists in 2^{M-1} different states.

[22] S. Milles, D. Mercadante, I. V. Aramburu, M. R. Jensen, N. Banterle, C. Koehler, S. Tyagi, J. Clarke, S. L. Shammas, M. Blackledge, F. Grater, and E. A. Lemke. Plasticity of an ultrafast interaction between nucleoporins and nuclear transport receptors. Cell **163** 734-745 (2015).

[23] M. Doi. *Soft Matter Physics*. Oxford University Press, Oxford (2013).

[24] A. Zilman, S. D. Talia, B. T. Chait, M. P. Rout and M. O. Magnasco. Efficiency, selectivity and robustness of nucleocytoplasmic transport. PLoS Comp. Biol. **3** e125 (2007).

[25] A stochastic process $X(t)$ is said to have the Markov property if the conditional probability distribution of future states of the process (conditional on both past and present states) depends only upon the present state, not on the sequence of events that preceded it. That is, for all $t' > t$ we have

$$\mathbb{P}[X(t') \leq x | X(s), s \leq t] = \mathbb{P}[X(t') \leq x | X(t)].$$

The strong Markov property is similar to the Markov property, except that the "present" is defined in terms of a stopping time. That is, given any finite-valued stopping time τ, if the stochastic process $Y(t) = X(t+\tau) - X(\tau)$ is independent of $\{X(s), s < \tau\}$ and has the same distribution as $\widehat{Y}(t) = X(t) - X(0)$ then X is said to satisfy the strong Markov property. Heuristically speaking, τ is a stopping time if for every t we can completely determine whether or not τ has occurred before time t using the statistical information known up to time t. A common example is a first passage time.

[26] J. Tetenbaum-Novatt, L. E. Hough, R. Mironska, A. S. McKenney, and M. P. Rout.Nucleocytoplasmic transport: A role for nonspecific competition in karyopherin-nucleoporin interactions. Mol. Cell. Proteomics **11** 31-46 (2012).